The 8th European Congress on Computational Methods in Applied Sciences and Engineering
ECCOMAS Congress 2022
5-–9 June 2022, Oslo, Norway

EFFICIENT STRATEGIES FOR SOLVING THE VARIABLE POISSON EQUATION WITH LARGE CONTRASTS IN THE COEFFICIENTS

Àdel Alsalti-Baldellou[1,2], Xavier Álvarez-Farré[1], Andrey Gorobets[3], F. Xavier Trias[1] and Assensi Oliva[1]

[1]Heat and Mass Transfer Technological Center, Technical University of Catalonia
Carrer de Colom 11, 08222 Terrassa (Barcelona), Spain; www.cttc.upc.edu
{adel.alsalti, xavier.alvarez.farre, francesc.xavier.trias, asensio.oliva}@upc.edu

[2]Termo Fluids SL
Carrer de Magí Colet 8, 08204 Sabadell (Barcelona), Spain; www.termofluids.com

[3] Keldysh Institute of Applied Mathematics, Russian Academy of Sciences
4A, Miusskaya Sq., Moscow 125047, Russia; www.keldysh.ru
andrey.gorobets@gmail.com

Key words: Poisson Equation, Reflection Symmetries, Multiphase Flow, Arithmetic Intensity

Abstract. Discrete versions of Poisson's equation with large contrasts in the coefficients result in very ill-conditioned systems. Thus, its iterative solution represents a major challenge, for instance, in porous media and multiphase flow simulations, where considerable permeability and density ratios are usually found. The existing strategies trying to remedy this are highly dependent on whether the coefficient matrix remains constant at each time iteration or not. In this regard, incompressible multiphase flows with high-density ratios are particularly demanding as their resulting Poisson equation varies along with the density field, making the reconstruction of complex preconditioners impractical. This work presents a strategy for solving such versions of the variable Poisson equation. Roughly, we first make it constant through an adequate approximation. Then, we block-diagonalise it through an inexpensive change of basis that takes advantage of mesh reflection symmetries, which are common in multiphase flows. Finally, we solve the resulting set of fully decoupled subsystems with virtually any solver. The numerical experiments conducted on a multiphase flow simulation prove the benefits of such an approach, resulting in up to 6.6x faster convergences.

1 INTRODUCTION

The principal bottleneck in the numerical simulation of many physical phenomena is the solution of Poisson's problem. For instance, linear elasticity, computational fluid dynamics (CFD), electro-magnetics, and groundwater flow simulations require the solution of large and sparse discrete versions of Poisson's equation. In its general form, it reads:

$$\nabla \cdot (\alpha \nabla u) = f \quad \text{in } \Omega, \tag{1}$$

where $\Omega \subseteq \mathbb{R}^3$ is an open and bounded domain on whose boundary, $\partial\Omega$, adequate boundary conditions are imposed.

As a result of their excessive memory and computational requirements, direct solvers [1] are generally unaffordable, and iterative alternatives such as Krylov subspace methods [2] are employed. However, their convergence rates highly depend on the spectrum of the linear systems' coefficient matrices. Then, ill-conditioned versions of the discrete Laplace operator, Δ, or, more generally, of $\nabla \cdot \alpha\nabla$, result in unacceptably slow convergences and require the use of robust preconditioners [3].

This work targets the solution of eq. (1) for large contrasts in the coefficients, α, which translate into very ill-conditioned systems. This is usually the case for porous media and multiphase flow simulations, where extreme permeability and density ratios are usually found. The existing strategies trying to remedy this are highly dependent on whether the coefficient matrix remains constant at each time iteration [4, 5] or not [6, 7]. In this regard, incompressible multiphase flows with high-density ratios are particularly challenging since their resulting Poisson equation varies along with the density field, making the reconstruction of complex preconditioners impractical.

This work presents a strategy for solving such versions of the variable Poisson equation. Roughly, we transform it into its constant counterpart through the approximation proposed by Dodd and Ferrante [7]. Then, we take advantage of mesh reflection symmetries, common in multiphase flows [8, 9, 10], to block-diagonalise it through an inexpensive change of basis. Finally, we solve concurrently the resulting set of fully decoupled subsystems with virtually any solver at a significantly lower computational cost.

The remaining sections are organised as follows. Section 2 introduces the governing equations for incompressible multiphase flow simulations. Additionally, it describes the approach for block-diagonalising the variable Poisson equation. Section 3 presents the test case and discusses the results obtained in the numerical experiments. Finally, section 4 gives some concluding remarks.

2 MATHEMATICAL FRAMEWORK

2.1 Governing equations

For simplicity, let us assume an incompressible two-phase flow of constant viscosity, μ, and densities ρ_1 and ρ_2. Such a flow is governed by the following version of the Navier-Stokes equations:

$$\frac{\partial \mathbf{v}}{\partial t} + (\mathbf{v} \cdot \nabla)\mathbf{v} = \frac{1}{\rho}\left(\mu\Delta\mathbf{v} - \nabla p + \sigma\kappa\delta_\Gamma\hat{\mathbf{n}}\right) \qquad (2)$$
$$\nabla \cdot \mathbf{v} = 0$$

where $\mathbf{v}$, p and ρ stand for the velocity, pressure and density fields, and σ, κ, δ_Γ and $\hat{\mathbf{n}}$ for the surface tension coefficient, interface curvature, Dirac delta and unit vector normal to the interface, respectively.

Then, a classical fractional step method is employed to solve the pressure-velocity coupling of eq. (2). It requires, at each time iteration, solving the following version of eq. (1):

$$\nabla \cdot \left(\frac{1}{\rho}\nabla p\right) = \frac{1}{\Delta t}\nabla \cdot \mathbf{v}^p \qquad (3)$$

for a given time-step, Δt.

A symmetry-preserving discretisation [11, 12, 13] of the system leads to the following discrete Navier-Stokes equations:

$$\Omega \frac{d\mathbf{v}_h}{dt} = -\mathsf{C}(\mathbf{v}_h)\mathbf{v}_h + \mathsf{N}\mathsf{D}\mathbf{v}_h - \mathsf{R}^{-1}\Omega\mathsf{G}p_h + \sigma\mathsf{K}\mathsf{G}\theta_h, \tag{4}$$

where C and D stand for the discrete convective and diffusive operators, K and θ_h for the discrete curvature [11] and level-set marker, and $\Omega = \mathrm{diag}(V_h)$, $\mathsf{N} = \mathrm{diag}(\mu/\rho_h)$ and $\mathsf{R} = \mathrm{diag}(\rho_h)$ are diagonal matrices accounting for the discrete mesh volume, kinematic viscosity, and density.

Then, the discrete gradient, G, and divergence, M, operators are related by:

$$\mathsf{G} = -\Omega^{-1}\mathsf{M}^t, \tag{5}$$

and, consequently, the discrete Laplace operator, $\mathsf{L} \coloneqq \mathsf{M}\mathsf{G}$, satisfies:

$$\mathsf{L} = -\mathsf{M}\Omega^{-1}\mathsf{M}^t. \tag{6}$$

Likewise, the discrete version of eq. (3) reads:

$$\hat{\mathsf{L}}p_h = \frac{1}{\Delta t}\mathsf{M}\mathbf{v}_h^p, \tag{7}$$

where we defined the *variable Laplace operator* as $\hat{\mathsf{L}} \coloneqq \mathsf{M}\mathsf{R}^{-1}\mathsf{G}$.

2.2 High density ratio Poisson's equation

As was already discussed, the main challenges in solving eq. (7) in the presence of large density ratios, ρ_2/ρ_1, are the severe ill-conditioning of the coefficient matrix, $\hat{\mathsf{L}}$, and the fact that it varies along with the density field, R.

Despite existing strategies to avoid reconstructing the preconditioners through inexpensive approximate updates [6], this work aims to study how to make the variable Poisson equation take advantage of spatial symmetries similarly to [14, 15]. To do so, we will rely on the approximation proposed by Dodd and Ferrante in [7]. Namely, letting $\rho_0 \coloneqq \min\{\rho_1, \rho_2\}$ and $\hat{p} \coloneqq 2p^n - p^{n-1}$, we will assume:

$$\frac{1}{\rho^{n+1}}\nabla p^{n+1} \simeq \frac{1}{\rho_0}\nabla p^{n+1} + \left(\frac{1}{\rho^{n+1}} - \frac{1}{\rho_0}\right)\nabla\hat{p}. \tag{8}$$

Then, combining eqs. (3) and (8):

$$\nabla^2 p = \frac{\rho_0}{\Delta t}\nabla\cdot\mathbf{v}^p + \nabla\cdot\left[\left(1 - \frac{\rho_0}{\rho}\right)\nabla\hat{p}\right], \tag{9}$$

or, in its discrete form:

$$\mathsf{L}p_h = \frac{\rho_0}{\Delta t}\mathsf{M}\mathbf{v}_h^p + \mathsf{M}\left(\mathbb{I} - \rho_0\mathsf{R}^{-1}\right)\mathsf{G}\hat{p}_h. \tag{10}$$

Applying the approximation of eq. (8) to replace eq. (7) with eq. (10) has two significant advantages. On the one hand, the coefficient matrix, L, is now constant. On the other, density contrasts no longer affect its conditioning.

Nevertheless, it is worth remarking that such an approach adds an artificial dissipation to the system. To see this, let us consider an inviscid two-phase flow free of surface tension, *i.e.*, with $\mu = 0$ and $\sigma = 0$. Then, the time derivative of the total kinetic energy, E_K, reads:

$$\frac{dE_K}{dt} = \left\langle \mathsf{R}\mathbf{v}_h, \frac{d\mathbf{v}_h}{dt} \right\rangle_\Omega, \tag{11}$$

which, by virtue of eq. (4), equals:

$$\frac{dE_K}{dt} = -\overbrace{\left\langle \mathsf{R}\mathbf{v}_h, \mathsf{C}(\mathbf{v}_h)\mathbf{v}_h \right\rangle_\Omega}^{dE_K/dt|_{\mathsf{C}(\mathbf{v}_h)}} - \overbrace{\left\langle \mathsf{R}\mathbf{v}_h, \mathsf{R}^{-1}\mathsf{G}p_h \right\rangle_\Omega}^{dE_K/dt|_{\nabla p}}. \tag{12}$$

Then, if we solve the more challenging eq. (7), *i.e.*, the variable Poisson equation, we have:

$$\left.\frac{dE_K}{dt}\right|_{\nabla p} = \left\langle \mathsf{R}\mathbf{v}_h, \mathsf{R}^{-1}\mathsf{G}p_h \right\rangle_\Omega = \langle \mathbf{v}_h, \mathsf{G}p_h \rangle_\Omega \overset{\text{eq. (5)}}{=} \left\langle \mathbf{v}_h, -\Omega^{-1}\mathsf{M}^t p_h \right\rangle_\Omega = \langle -\mathsf{M}\mathbf{v}_h, p_h \rangle = 0, \tag{13}$$

given that $\mathsf{M}\mathbf{v}_h = \mathbf{0}_h$.

Conversely, if we use the approximation of eq. (8) to solve the easier eq. (10), *i.e.*, the constant Poisson equation, we have:

$$\left.\frac{dE_K}{dt}\right|_{\nabla p} \overset{\text{eq. (8)}}{=} \left\langle \mathsf{R}\mathbf{v}_h, \frac{1}{\rho_0}\mathsf{G}p_h + \mathsf{R}^{-1}\mathsf{G}\hat{p}_h - \frac{1}{\rho_0}\mathsf{G}\hat{p}_h \right\rangle_\Omega = \tag{14}$$

$$= \left\langle \frac{1}{\rho_0}\mathsf{R}\mathbf{v}_h, \mathsf{G}\left(p_h - \hat{p}_h\right) \right\rangle_\Omega + \langle \mathbf{v}_h, \mathsf{G}\hat{p} \rangle_\Omega \overset{\text{eq. (5)}}{=} \left\langle \frac{1}{\rho_0}\mathsf{R}\mathbf{v}_h, \mathsf{G}\left(p_h - \hat{p}_h\right) \right\rangle_\Omega - \langle \mathsf{M}\mathbf{v}_h, p_h \rangle .$$

Remarkably enough, it is no longer guaranteed that $\mathsf{M}\mathbf{v}_h = \mathbf{0}_h$. Additionally, the more inaccurate the interpolated pressure, $\hat{p}_h$, is, the more unphysical the kinetic energy becomes. Similarly, the larger the density ratio, ρ_1/ρ_2, the higher the impact of this artificial perturbation.

2.3 Benefiting from mesh symmetries

For clarity, let us consider a (structured or unstructured) mesh with a single reflection symmetry, *i.e.*, a mesh analogous to fig. 1. Additionally, let us impose the same grid points' ordering on each side. As a result, the entire mesh is halved into two subdomains, and all the scalar fields satisfy:

$$\mathbf{x} = \begin{pmatrix} \mathbf{x}_1 \\ \mathbf{x}_2 \end{pmatrix} \in \mathbb{R}^n, \tag{15}$$

where n stands for the mesh size and $\mathbf{x}_1, \mathbf{x}_2 \in \mathbb{R}^{n/2}$ for $\mathbf{x}$'s restriction to each of the subdomains. Furthermore, spatially symmetric points are in the same position within the subvectors, and the discrete Laplace operator satisfies:

$$\mathsf{L} = \begin{pmatrix} \mathsf{L}_{\text{inn}} & \mathsf{L}_{\text{out}} \\ \mathsf{L}_{\text{out}} & \mathsf{L}_{\text{inn}} \end{pmatrix} \in \mathbb{R}^{n \times n}, \tag{16}$$

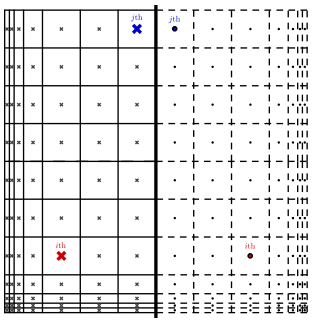

Figure 1: The single-symmetry case.

where $\mathsf{L}_{\text{inn}}, \mathsf{L}_{\text{out}} \in \mathbb{R}^{n/2 \times n/2}$ correspond to the inner- and outer-subdomain couplings, respectively.

Then, we can define the following change-of-basis:

$$\mathsf{S} := \frac{1}{\sqrt{2}} \begin{pmatrix} \mathbb{I}_{n/2} & \mathbb{I}_{n/2} \\ \mathbb{I}_{n/2} & -\mathbb{I}_{n/2} \end{pmatrix} \in \mathbb{R}^{n \times n}, \tag{17}$$

which satisfies $\mathsf{S}^{-1} = \mathsf{S}$, and block-diagonalises L:

$$\mathsf{S}\mathsf{L}\mathsf{S}^{-1} = \begin{pmatrix} \mathsf{L}_{\text{inn}} + \mathsf{L}_{\text{out}} & 0 \\ 0 & \mathsf{L}_{\text{inn}} - \mathsf{L}_{\text{out}} \end{pmatrix}, \tag{18}$$

transforming eq. (10) into two decoupled and half-sized subsystems.

More generally, on meshes with s symmetries we can apply the steps above recursively and decompose L into 2^s decoupled subsystems, $\mathsf{L}_{s_1}, \ldots, \mathsf{L}_{s_{2^s}}$, of size $n/2^s$:

$$\mathsf{L}_s \leftarrow \begin{pmatrix} \mathsf{L}_{s_1} & & 0 \\ & \ddots & \\ 0 & & \mathsf{L}_{s_{2^s}} \end{pmatrix}$$

thus replacing eq. (10) with:

$$\mathsf{L}_s \left(\mathsf{S} p_h\right) = \mathsf{S} \left(\frac{\rho_0}{\Delta t} \mathsf{M} v_h^p + \mathsf{M} \left(\mathbb{I} - \rho_0 \mathsf{R}^{-1} \right) \mathsf{G} \hat{p}_h \right). \tag{19}$$

Algorithm 1 summarises the resulting strategy.

Algorithm 1 Poisson solver exploiting s reflection symmetries

Require: $\mathsf{L} \in \mathbb{R}^{n \times n}$ and $\mathbf{b} \in \text{Range}(\mathsf{L}) \subseteq \mathbb{R}^{n \times n}$

1: **procedure** SOLVE($\mathbf{b}, \mathsf{L}_s$)
2: Transform forward the right-hand side: $\mathbf{b}' = \mathsf{S}\mathbf{b}$
3: Decoupled solution of the 2^s subsystems: $\mathsf{L}_{s_1}\mathbf{x}'_1 = \mathbf{b}'_1, \ldots, \mathsf{L}_{s_{2^s}}\mathbf{x}'_{2^s} = \mathbf{b}'_{2^s}$
4: Transform backward the solution: $\mathbf{x} = \mathsf{S}^{-1}\mathbf{x}'$
5: **end procedure**

3 NUMERICAL EXPERIMENTS

The test case considered is a two-phase flow relying on the symmetry-preserving staggered discretisation of [11]. It consists of an initially static ellipse, fig. 2a, moved by the surface tension action to the evolved state on which we have conducted all the numerical experiments, fig. 2b. Table 1 summarises the idealised parameters considered. Remarkably enough, exploiting symmetries naturally applies to arbitrary unstructured meshes. However, for the sake of simplicity, in the present work we have only considered Cartesian uniform grids, thus having: $\Omega = \Delta x \Delta y \mathbb{I}_n$.

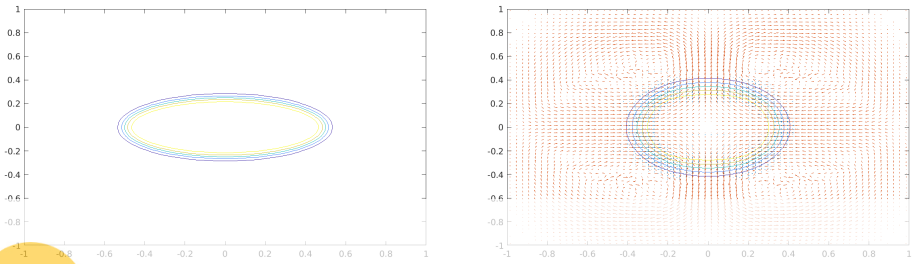

(a) Initial configuration (b) Evolved configuration

Figure 2: Two-phase flow test case.

Parameter		Units	Internal fluid	External fluid
Density	ρ	Kg/m^3	$\rho_1 = 1.0$	$\rho_2 = ratio^{-1}$
Dynamic viscosity	μ	Ns/m^2	10^{-4}	
Surface tension coefficient	σ	N/m	$\rho_2/1000$	
Initial ellipse axes	$(a,\ b)$	m	$(1.0,\ 0.5)$	

Table 1: Idealised parameters defining the two-phase flow test case.

Figure 3 illustrates the impact of the density ratio on $\hat{\mathsf{L}}$'s conditioning. As expected, large density ratios result in extremely ill-conditioned (variable) systems.

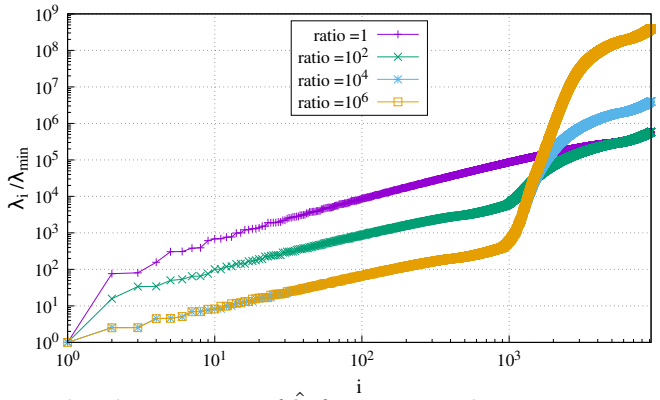

Figure 3: Normalised spectrum of $\hat{\mathsf{L}}$ for various density ratios on a 96^2 mesh.

Label	Case
Lap	Equation (7)
DF	Equation (10)
DF + 1sym	Equation (19), $s = 1$
DF + 2sym	Equation (19), $s = 2$

Table 2: Labels used in the convergence plots.

In order to illustrate the effect of exploiting mesh symmetries, we have solved eqs. (7), (10) and (19) using different density ratios. Table 2 summarises the labels used in the convergence plots to identify each of the equations solved. The solvers considered are differently preconditioned Conjugate Gradient methods (PCG). Additionally, we have utilised the last time iteration's pressure field as the initial guess for the solvers in order to accelerate their convergence.

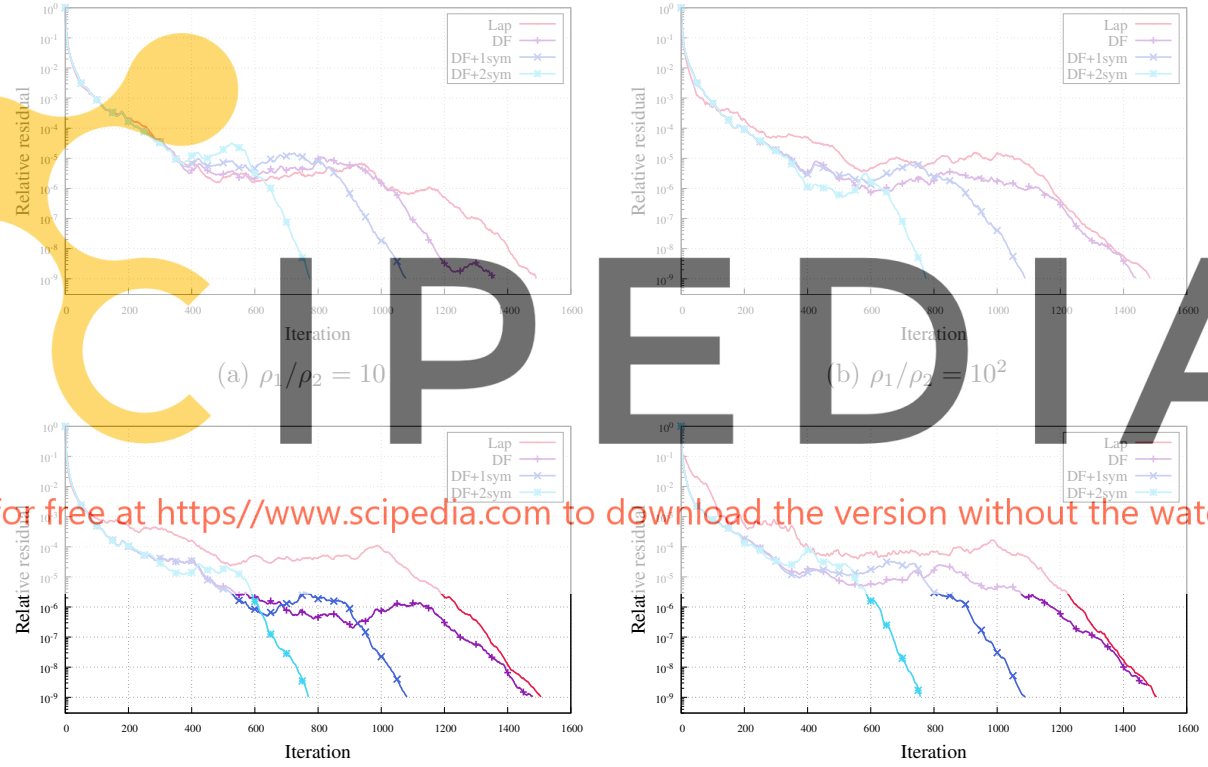

(a) $\rho_1/\rho_2 = 10$ (b) $\rho_1/\rho_2 = 10^2$

(c) $\rho_1/\rho_2 = 10^3$ (d) $\rho_1/\rho_2 = 10^6$

Figure 4: Jacobi preconditioned CG convergence for various density ratios on a 256^2 mesh.

The preconditioners considered are Jacobi, Incomplete Cholesky (IC) [16] and the sparse approximate inverse (SPAI) of Grote and Huckle [17]. Despite Jacobi's relatively low impact on the system's conditioning, its simplicity makes it the only one suitable (at least, "as it is") for the variable case, *i.e.*, for eq. (7). Indeed, not only reconstructing more complex preconditioners

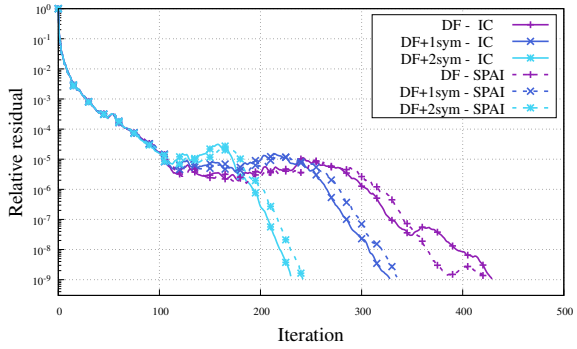

(a) $\rho_1/\rho_2 = 10$

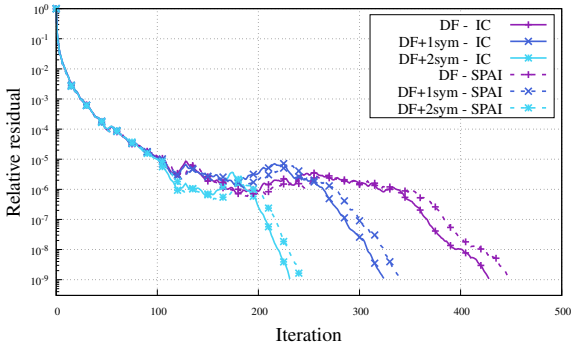

(b) $\rho_1/\rho_2 = 10^2$

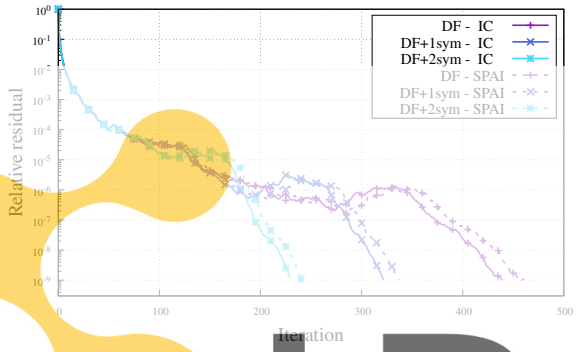

(c) $\rho_1/\rho_2 = 10^3$

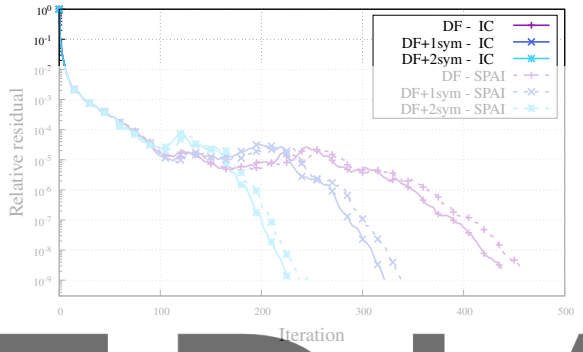

(d) $\rho_1/\rho_2 = 10^6$

Figure 5: IC and SPAI preconditioned CG convergence for various density ratios on a 256^2 mesh.

at each time iteration is computationally unaffordable, but also, in most real simulations, the variable coefficient matrix, $\hat{\mathsf{L}} = \mathsf{M}\mathsf{R}^{-1}\mathsf{G}$, is only available in its factored form.

Two points can be inferred from fig. 4. On the one hand, if the preconditioners' reconstruction were not an issue (and, therefore, having a constant coefficient matrix was not a substantial benefit), it would not be worth replacing eq. (7) with eq. (10) at the cost of the artificial dissipation added by eq. (8). On the other hand, it becomes clear that even with such a simple preconditioner and regardless of the density ratio, exploiting symmetries and solving the alternative eq. (19) greatly accelerates the solvers' convergence.

Regarding fig. 5, the advantages of using eq. (8) to make the variable Poisson equation constant are evident. Indeed, using more complex preconditioners such as IC or SPAI leads to substantially faster convergences. On top of that, exploiting symmetries further improves the solvers' performance. For instance, exploiting two symmetries and using an IC preconditioned PCG to solve eq. (19) results in up to 2.0x faster convergences than solving eq. (10) with the same solver and up to 6.6x compared to solving eq. (7) with a Jacobi preconditioned PCG.

4 CONCLUSIONS

In this work, we have presented a strategy to accelerate the solution of the variable coefficients Poisson equation. We have focused on the multiphase flow case, which usually presents mesh symmetries and whose large density contrasts lead to extremely ill-conditioned (and variable) linear systems. Hence, we have recalled the approximation due to Dodd and Ferrante [7] to make constant the coefficient matrix. It allowed us to extend to the variable case a strategy for exploiting mesh symmetries in the solution of Poisson's equation [14, 15].

On the one hand, the overhead of our strategy is minimal given the negligible cost of the two transforms involved. On the other, the numerical experiments presented confirm that benefiting from mesh symmetries to solve the equivalent eq. (19) accelerates the convergence of the iterative methods up to 2.0x and 6.6x with respect to solving the alternative eqs. (7) and (10), respectively.

Future lines of work include evaluating the current strategy on an actual simulation code following an algebra-based approach [18]. Hence, we plan to implement it within our in-house code [19, 20], and expect not only to attain great accelerations on the Poisson solvers but also to benefit from other computational advantages. Namely, the regular block structure of virtually all the operators allows replacing all the sparse matrix-vector products with the higher arithmetic intensity sparse matrix-dense matrix product. As a result, we will accelerate all matrix multiplications and reduce the simulation's memory footprint.

ACKNOWLEDGEMENTS

Àdel Alsalti-Baldellou, Xavier Álvarez-Farré, F. Xavier Trias and Assensi Oliva have been financially supported by two competitive R+D projects: RETOtwin (PDC2021-120970-I00), given by MCIN/AEI/10.13039/501100011033 and European Union Next GenerationEU/PRTR, and FusionCAT (001-P-001722), given by *Generalitat de Catalunya* RIS3CAT-FEDER. Àdel Alsalti-Baldellou has also been supported by the predoctoral grants DIN2018-010061 and 2019-DI-90, given by MCIN/AEI/10.13039/501100011033 and the Catalan Agency for Management of University and Research Grants (AGAUR), respectively. Andrey Gorobets has been supported by the RSF project 19-11-00249.

REFERENCES

[1] P. R. Amestoy, A. Buttari, J.-Y. L'Excellent, and T. Mary, "Performance and Scalability of the Block Low-Rank Multifrontal Factorization on Multicore Architectures," *ACM Trans. Math. Softw.*, vol. 45, pp. 1–26, mar 2019.

[2] H. A. van der Vorst, *Iterative Krylov Methods for Large Linear Systems*, vol. 56. Cambridge University Press, apr 2003.

[3] M. Ferronato, "Preconditioning for Sparse Linear Systems at the Dawn of the 21st Century: History, Current Developments, and Future Perspectives," *ISRN Appl. Math.*, vol. 2012, pp. 1–49, dec 2012.

[4] G. Diaz Cortes, C. Vuik, and J. Jansen, "On POD-based Deflation Vectors for DPCG applied to porous media problems," *J. Comput. Appl. Math.*, vol. 330, pp. 193–213, mar 2018.

[5] R. Scheichl and E. Vainikko, "Additive Schwarz with aggregation-based coarsening for elliptic problems with highly variable coefficients," *Computing*, vol. 80, pp. 319–343, sep 2007.

[6] À. Alsalti-Baldellou, F. X. Trias, A. Gorobets, and A. Oliva, "On Preconditioning Variable Poisson Equation with Extreme Contrasts in the Coefficients," in *14th WCCM-ECCOMAS Congr.*, no. January, pp. 11–15, CIMNE, 2021.

[7] M. S. Dodd and A. Ferrante, "A fast pressure-correction method for incompressible two-fluid flows," *J. Comput. Phys.*, vol. 273, pp. 416–434, sep 2014.

[8] N. Valle, *On the development of direct numerical simulations for falling films*. PhD thesis, Universitat Politècnica de Catalunya - BarcelonaTech, 2021.

[9] A. Amani, E. Schillaci, D. Kizildag, and C.-D. Pérez-Segarra, "Numerical Analysis of Viscoelastic Fluid Injection Processes," in *14th WCCM-ECCOMAS Congr.*, CIMNE, 2021.

[10] A. Amani, N. Balcázar, E. Gutiérrez, and A. Oliva, "Numerical study of binary droplets collision in the main collision regimes," *Chem. Eng. J.*, vol. 370, pp. 477–498, aug 2019.

[11] N. Valle, F. X. Trias, and J. Castro, "An energy-preserving level set method for multiphase flows," *J. Comput. Phys.*, vol. 400, p. 108991, jan 2020.

[12] F. X. Trias, O. Lehmkuhl, A. Oliva, C.-D. Pérez-Segarra, and R. W. C. P. Verstappen, "Symmetry-preserving discretization of Navier-Stokes equations on collocated unstructured grids," *J. Comput. Phys.*, vol. 258, pp. 246–267, feb 2014.

[13] R. W. Verstappen and A. E. Veldman, "Symmetry-preserving discretization of turbulent flow," *J. Comput. Phys.*, vol. 187, no. 1, pp. 343–368, 2003.

[14] A. Gorobets, F. X. Trias, R. Borrell, O. Lehmkuhl, and A. Oliva, "Hybrid MPI+OpenMP parallelization of an FFT-based 3D Poisson solver with one periodic direction," *Comput. Fluids*, vol. 49, no. 1, pp. 101–109, 2011.

[15] O. Shishkina, A. Shishkin, and C. Wagner, "Simulation of turbulent thermal convection in complicated domains," *J. Comput. Appl. Math.*, vol. 226, pp. 336–344, apr 2009.

[16] J. A. Meijerink and H. A. van der Vorst, "An iterative solution method for linear systems of which the coefficient matrix is a symmetric M-matrix," *Math. Comput.*, vol. 31, no. 137, pp. 148–162, 1977.

[17] M. J. Grote and T. Huckle, "Parallel Preconditioning with Sparse Approximate Inverses," *SIAM J. Sci. Comput.*, vol. 18, pp. 838–853, may 1997.

[18] N. Valle, X. Álvarez-Farré, A. Gorobets, J. Castro, A. Oliva, and F. Xavier Trias, "On the implementation of flux limiters in algebraic frameworks," *Comput. Phys. Commun.*, vol. 271, p. 108230, 2022.

[19] X. Álvarez-Farré, A. Gorobets, and F. X. Trias, "A hierarchical parallel implementation for heterogeneous computing. Application to algebra-based CFD simulations on hybrid supercomputers," *Comput. Fluids*, vol. 214, p. 104768, jan 2021.

[20] X. Álvarez-Farré, A. Gorobets, F. X. Trias, R. Borrell, and G. Oyarzun, "HPC^2 – A fully-portable, algebra-based framework for heterogeneous computing. Application to CFD," *Comput. Fluids*, vol. 173, pp. 285–292, sep 2018.